Predicting N_2O emissions from nitrifying and denitrifying biofilms: a modeling study

Fabrizio Sabba, Cristian Picioreanu, Joshua P. Boltz and Robert Nerenberg

ABSTRACT

Wastewater treatment plants can be significant sources of nitrous oxide (N_2O), a potent greenhouse gas. While our understanding of N_2O emissions from suspended-growth processes has advanced significantly, less is known about emissions from biofilm processes. Biofilms may behave differently due to their substrate gradients and microbial stratification. In this study, we used mathematical modeling to explore the mechanisms of N_2O emissions from nitrifying and denitrifying biofilms. Our ammonia-oxidizing bacteria biofilm model suggests that N_2O emissions from biofilm can be significantly greater than from suspended-growth systems. The driving factor is the diffusion of hydroxylamine, a nitrification intermediate, from the aerobic to the anoxic regions of the biofilm. The presence of nitrite-oxidizing bacteria further increased emissions. For denitrifying biofilms, our results suggest that emissions are generally greater than for suspended-growth systems. However, the magnitude of the difference depends on the bulk dissolved oxygen, chemical oxygen demand, and nitrate concentrations, as well as the biofilm thickness. Overall, the accumulation and diffusion of key intermediates, i.e. hydroxylamine and nitrite, distinguish biofilms from suspended-growth systems. Our research suggests that the mechanisms of N_2O emissions from biofilms are much more complex than suspended-growth systems, and that emissions may be higher in many cases.

Key words | biofilm, denitrification, electron mediators, nitrification, N_2O emissions

Fabrizio Sabba
Robert Nerenberg (corresponding author)
Department of Civil and Environmental Engineering and Earth Science,
University of Notre Dame,
156 Fitzpatrick Hall,
Notre Dame,
IN 46556,
USA
E-mail: *rnerenbe@nd.edu*

Cristian Picioreanu
Department of Biotechnology, Faculty of Applied Sciences,
Delft University of Technology,
Julianalaan 67,
Delft 2628 BC,
The Netherlands

Joshua P. Boltz
8922 Green Valley Drive,
Theodore,
AL 36582,
USA

INTRODUCTION

Nitrous oxide (N_2O) is a potent greenhouse gas, with a global warming potential 300 times greater than that of CO_2 (IPCC 2013). Wastewater treatment plants can be an important source of N_2O (Ahn *et al.* 2010). Emissions from wastewater may result from incomplete denitrification (Kampschreur *et al.* 2009; Lu & Chandran 2010; Pan *et al.* 2012), but also from nitrification (Tallec *et al.* 2006; Kampschreur *et al.* 2008, Kampschreur *et al.* 2009; Lu & Chandran 2010; Wunderlin *et al.* 2012; Ye *et al.* 2014; Daelman *et al.* 2015). During nitrification, N_2O emissions may result from nitrifier denitrification as well as chemical degradation of hydroxylamine (NH_2OH) (Schreiber *et al.* 2009, 2012; Harper *et al.* 2015; Soler-Jofra *et al.* 2016).

While extensive research has investigated N_2O formation in suspended-growth systems (Kimochi *et al.* 1998; Colliver & Stephenson 2000; Kampschreur *et al.* 2008; Ahn *et al.* 2010; Lu & Chandran 2010; Aboobakar *et al.* 2013), few studies have explored its formation in biofilm-based processes, such as the moving bed biofilm reactor, biological aerated filter, and granular sludge. Such processes have been gaining in popularity, and therefore it is important to understand their potential for N_2O emissions.

Bacteria in suspended-growth systems are directly exposed to the bulk liquid. Thus, the formation of N_2O depends exclusively on the conditions in the bulk environment. For example, little or no N_2O formation would be expected from denitrifying bacteria if the bulk is fully aerobic, as denitrification would be inhibited by O_2. In a biofilm, however, O_2 gradients exist. Even if the bulk liquid were aerobic, bacteria in the deeper biofilm could experience anoxic conditions, allowing nitrate reduction and the formation of N_2O.

A number of models have been developed to predict N_2O formation by nitrifying (Kampschreur *et al.* 2007, 2008; Ni *et al.* 2011; Mampaey *et al.* 2013; Ni *et al.* 2013, 2014) and denitrifying microorganisms (Hiatt & Grady 2008; Ni *et al.* 2011; Kampschreur *et al.* 2012; Pan *et al.* 2013). In particular, recent models have improved the prediction of N_2O by

doi: 10.2166/wst.2016.484

explicitly considering formation and consumption of nitrification and denitrification intermediates, and modeling the competition of key enzymes for intracellular electron mediators (Pan *et al.* 2013; Ni *et al.* 2014; Ni & Yuan 2015). A recent study used such a model to predict the mechanisms of N_2O formation from nitrifying biofilms containing ammonia-oxidizing bacteria (AOB) (Sabba *et al.* 2015). However, this study did not consider the effects of nitrite-oxidizing bacteria (NOB) in nitrifying biofilms, nor did it assess the effects of gas stripping, e.g. via aeration. More importantly, there are no studies addressing the mechanisms of N_2O formation from denitrifying biofilms.

The objective of this study was to use mathematical modeling to systematically explore N_2O production and emissions from nitrifying and denitrifying biofilms. Note that we use the words N_2O *production* (the net formation of N_2O from the biofilm) and *emissions* (loss of N_2O from the reactor in liquid and gas phases) interchangeably in this paper. Also, the intent was not to accurately predict N_2O emissions, but to explain how the mechanisms of N_2O formation in biofilm differ from those from in suspended growth systems. We assessed N_2O emissions from nitrifying biofilms consisting solely of AOB, or AOB plus NOB. Denitrifying biofilms were studied separately, to clearly establish the mechanisms of N_2O formation by each population.

METHODS

The biofilm models used to predict N_2O production in biofilms were based on traditional diffusion-reaction mass balances for the relevant chemical species in both nitrifying and denitrifying biofilms.

The nitrifying model considered N_2O formation by AOB via two pathways: the hydroxylamine (NH_2OH) pathway and the nitrifier denitrification pathways. This approach is based on a recently published model (Ni *et al.* 2014; Sabba *et al.* 2015). While in our previous work we focused on the mechanisms of N_2O formation in biofilms consisting exclusively of AOB (Sabba *et al.* 2015), in this work we expanded on the previous work and explored the effects of gas stripping and of the combined presence of AOB and NOB within the biofilm. Furthermore, we studied the mechanisms of N_2O emissions in denitrifying biofilms, with and without gas stripping.

Parameters for the nitrification model are reported in Table 1. While a base AOB density, assuming uniform distribution of AOB, was used in most studies, different biomass densities were also tested. For additional tests with AOB along with a constant and uniformly distributed population of NOB, the NOB were simulated using the conventional ASM model, i.e. without electron mediators (Picioreanu *et al.* 1997). The denitrifying model included N_2O formation by heterotrophic bacteria, and was adapted from Pan *et al.* (2013).

A continuous, ideally-mixed biofilm reactor incorporating nitrifying or heterotrophic bacteria was modeled. The two separate models evaluated one-dimensional, planar biofilms. A hydraulic retention time of 6 hours for the nitrifying and 1.5 hours for the denitrifying condition was used. As initial values, all concentrations in biofilm and bulk liquid were taken as equal to the corresponding influent concentrations. As base condition, a biofilm specific surface area of 125 m^2 m^{-3} was used. Biomass growth, decay, attachment and detachment were not considered. Biofilms of different thicknesses were modeled. Thicknesses of 2 μm for the nitrifying and 5 μm for the denitrifying biofilm were assumed to represent 'suspended growth'. While these thicknesses were chosen arbitrarily, they both had essentially had no substrate gradients within the depth and therefore behaved as suspended growth.

For the denitrification process, O_2, nitrite (NO_2^-), nitric oxide (NO), N_2O, nitrate (NO_3^-) and chemical oxygen demand (COD) were included as state variables. Note that the COD is assumed to be readily biodegradable. For the nitrification process, the model additionally considered ammonia (NH_3) and NH_2OH as state variables, but did not include COD. The conditions tested in both models are listed in Tables 1 and 2. All model equations and process matrices are provided in the Supporting Information in Tables S1–S3 for the nitrifying model and Tables S4–S6 for the denitrifying model (the Supporting Information is available with the online version of this paper). The denitrification model was used to predict the effects of bulk O_2 and NO_3^- concentrations on N_2O production in denitrifying biofilms, assuming an influent NO_3^- concentration of 14 mgN L^{-1}. The bulk COD concentration was 720 mgCOD L^{-1}, such that COD was not rate limiting within the biofilm. The assessed biofilm thicknesses were 5, 50 and 400 μm. In the denitrification model, we added an O_2 reduction process with a high maximum reduction rate, q_{max}, and a very high relative affinity for M_{red} such that O_2 reduction was prioritized over denitrification. This novel approach to modeling O_2 inhibition guarantees that, as long as O_2 is present, it will keep M_{red} at very low levels and inhibit the reduction of nitrogen oxides. This approach is a more fundamental alternative to the conventional 'oxygen switch' used in the ASM models, and allows the distinct inhibitory effect of O_2 on each enzyme to be included via the M_{red} concentration.

Most modeling runs were without N_2O stripping. However, for some runs we explored the effects of stripping on N_2O emissions. As NO usually does not accumulate and

Table 1 | Parameters used for the nitrification model

Parameter	Symbol	Value	Units	Source
Concentrations in influent				
Oxygen	$C_{in,O2}$	from 0.001 to 5 (varied)	mg L^{-1}	Typical range
Ammonia	$C_{in,NH3}$	80	mgN L^{-1}	Chosen
Hydroxylamine, nitrous oxide, nitric oxide, nitrite, nitrate	$C_{in,i}$	0	mgN L^{-1}	Chosen
Initial concentrations	$C_{0,i}$	$C_{in,i}$	mgO_2 L^{-1}	Chosen
Biomass concentration in the biofilm				
Ammonia oxidizers, AOB	$C_{F,XAOB}$	50 (base case) 50 or 35 (with NOB)	g L^{-1}	Typical value, Wanner *et al.* (2006)
Nitrite oxidizers, NOB	$C_{F,XNOB}$	0 (base case) 15 (with NOB)	g L^{-1}	Picioreanu *et al.* (1997)
Concentration total redox mediators	$C_{T,Med}$	0.01	mol kg^{-1}	Ni *et al.* (2014)
Biofilm thickness	L_F	100 (base case) 2, 50, 100 (varied)	μm	Typical values
Liquid flow rate	Q	11	mL min^{-1}	Chosen
Liquid volume in the reactor	V_B	4	L	Chosen
Biofilm surface area	A_F	0.5	m^2	Chosen
Gas volume	V_G	3.5	L	Chosen
Gas flow rate	Q_G	2	L min^{-1}	Chosen
Gas-liquid mass transfer coeff.	k_La	100	h^{-1}	Chosen
Henry gas-liquid coefficient N_2O (25 °C)	H_{N2O}	0.611	mol mol^{-1}	*CRC Handbook* (2014)

Table 2 | Parameters used for the denitrification model

Parameter	Symbol	Value	Units	Source
Concentrations in influent				
Methanol (as COD)	$C_{0,COD}$	720 (non-limiting)	mg L^{-1}	Chosen
Nitrate	$C_{0,NO3}$	Range 0.0001–50	mg L^{-1}	Varied
Nitrite	$C_{0,NO2}$	0	mgN L^{-1}	Chosen
Nitric oxide	$C_{0,NO}$	0	mgN L^{-1}	Chosen
Nitrous oxide	$C_{0,N2O}$	0	mgN L^{-1}	Chosen
Oxygen	$C_{0,O2}$	Range 0.00001–4	mgO_2 L^{-1}	Varied
Biomass concentration in the biofilm				
Concentration total redox mediators	$C_{T,Med}$	0.01	mol kg^{-1}	Pan *et al.* (2013)
Biofilm thickness	L_F	400 (base case) 5, 50, 400 (varied)	μm	Typical values
Liquid flow rate	Q	44	mL min^{-1}	Chosen
Liquid volume in the reactor	V_b	4	L	Chosen
Biofilm surface area	A_F	0.5	m^2	Chosen
Gas volume	V_G	3.5	L	Chosen
Gas flow rate	Q_G	2	L min^{-1}	Chosen
Gas-liquid mass transfer coeff.	k_La	100	h^{-1}	Chosen
Henry gas-liquid coefficient N_2O (25 °C)	H_{N2O}	0.611	mol mol^{-1}	*CRC Handbook* (2014)

acts as a transient compound, its stripping was not included in the model. To simulate N_2O stripping during aeration, an additional transfer term was included in the liquid N_2O mass balance as $k_La\,(C_{G,N_2O}H_{N_2O} - C_{B,N_2O})$, and a further equation was solved for the gas phase concentration, $C_{G,N2O}$ (mol/m^3 gas), as $dC_{G,N_2O}/dt = Q_G/V_G(0-C_{G,N_2O})-k_La(C_{G,N_2O}H_{N_2O}-C_{B,N_2O})$.

The model was implemented on the COMSOL Multiphysics platform. Equations for one-dimensional diffusion and reaction, for a fixed biofilm density and thickness, were solved with variable time step on a biofilm domain discretized with a mesh size of 1 μm. Steady state was assumed to be reached when effluent concentrations were stable. Steady state for all conditions was obtained after maximum simulation time of three days for nitrifying biofilms and one day for heterotrophic biofilms.

A summary of the nitrifying and denitrifying conditions used for the model can be found in Tables 1 and 2, respectively. A complete list of stoichiometric matrices, reaction rates and other model parameters for both models can be found in the Supporting Information (Tables S1–S6).

RESULTS AND DISCUSSION

Nitrifying biofilms

Effect of O_2 and thickness on N_2O emissions

We first explored N_2O emissions from an AOB biofilm as a function of bulk O_2 for biofilm thicknesses of 2, 50, and 100 μm. We then selected one biofilm thickness, 100 μm, and analyzed its behavior in more detail. Finally we evaluated the effects of NOB on the overall N_2O emissions.

The nitrifying model suggests that thicker biofilms have greater N_2O emissions than thin biofilms, which represent suspended-growth systems (Figure 1(a)). A range of thicknesses was simulated. The emission rates increased with increasing in O_2. However, this behavior was different for thinner biofilms and suspended growth systems, where N_2O reached its maximum at much lower O_2 levels than for thicker biofilms. Biofilms with greater thicknesses (e.g. 50 and 100 μm) followed similar general trends with regards to N_2O emissions (Figure 1(a)). This trend confirmed that thicker biofilms not only had higher emissions, but also had N_2O emissions for a much wider range of O_2 values. The main cause is the diffusion of NH_2OH, an AOB nitrification intermediate. Diffusion of reaction intermediates has been previously shown (De Beer *et al.* 1997; Stewart 2003; Sabba *et al.* 2015). NH_2OH forms in the outer, aerobic regions of the biofilm and diffuses to the inner, anoxic regions of the biofilm (Figure 1(b)). The higher emissions for thicker biofilms occurred on a basis of a higher biomass content for biofilms, respectively.

To better understand and explore the mechanisms that lead to N_2O formation, a base case of a 100-μm biofilm was considered (Figure 1(b)). Figure 1(b) shows the net rates of formation or consumption of nitrifying key species and O_2. In a suspended-growth system at steady state, the rate of NH_3 oxidation should equal the rate of NH_2OH oxidation. In biofilms, however, some NH_2OH may diffuse into the deeper portions of the biofilm, resulting in a net formation of NH_2OH in the outer biofilm and net consumption in the interior (Figure 1(b)).

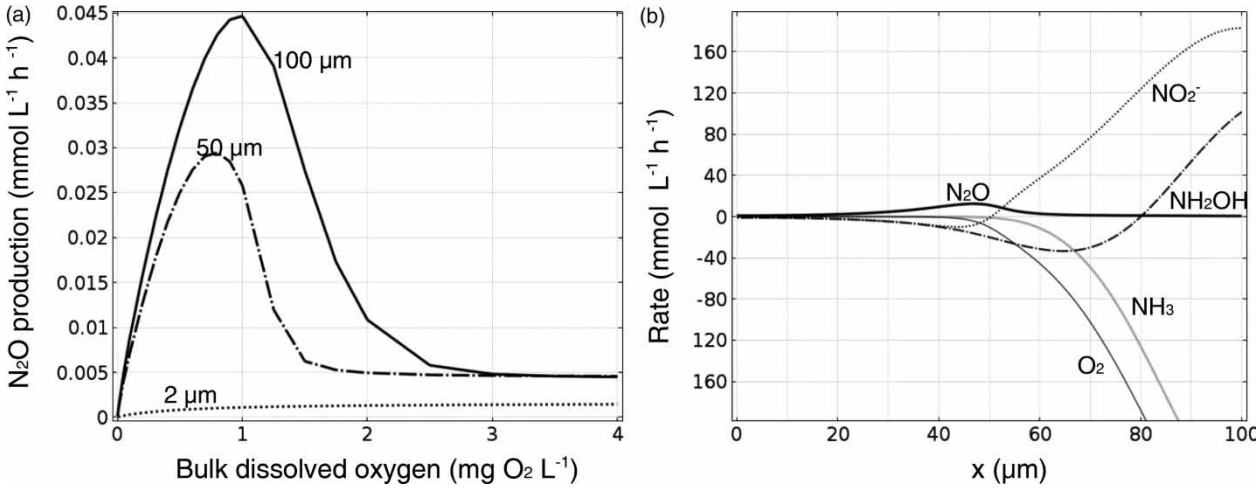

Figure 1 | (a) N_2O production rates for AOB biofilms of different thicknesses with a constant biofilm surface area, per unit reactor volume, as a function of bulk O_2, and (b) net component rates over the biofilm depth (x) for the 100-μm biofilm. Results are for the base case conditions at a bulk O_2 of 0.9 mg L^{-1}.

The external portion of the biofilm (right side of Figure 1(b)) has high nitrification rates due to the high concentrations of NH_3 and O_2. This can be seen in Figure 1(b), where there is net consumption of both compounds and net formation of NH_2OH and NO_2^- as products. Essentially, all of the electrons from NH_2OH oxidation are utilized for O_2 reduction in this zone, allowing little NO_2^- reduction. However, at greater depths, around 60 μm, O_2 becomes limiting and the rate of NH_3 consumption approaches zero. In this zone, little NH_3 reduction takes place, but electrons produced from NH_2OH that diffuses from the outer layers are used for NO_2^- reduction, leading to a spike in N_2O formation. Below 30 μm, NH_2OH is no longer available and the rate of N_2O formation decreases to zero. This is also true for larger thicknesses where different biomass concentrations might be present. With increasing thicknesses, the inner portions become inactive, while the amount of active biomass close to the bulk liquid remains similar. The NH_2OH pathway contributed only to a small extent to the N_2O overall production, while the nitrifier denitrification pathway was the main contributor for most of the N_2O produced. These results are similar to those found by Sabba *et al.* (2015).

Effect of NOB on N_2O emissions

Sabba *et al.* (2015) studied a biofilm consisting solely of AOB. However, nitrifying biofilms commonly typically include both AOB and NOB. While NOB do not directly produce N_2O, they may affect N_2O formation by AOB by modifying the surrounding environment.

If the total density of AOB only is 50 g L^{-1} (base case), and NOB provide an additional 15 g L^{-1} density for a total of 65 g L^{-1}, the N_2O emissions increase with respect to the base case (Figure 2). This is because a higher overall biomass density of AOB and NOB leads to higher O_2 gradients in the biofilm. This promotes a higher gradient of NH_3 oxidation rates and O_2 concentrations, leading to greater diffusion of NH_2OH into the deeper biofilm. It also contributes to the formation of an anoxic zone within the biofilm depth.

Interestingly, even if the AOB density drops to 35 g L^{-1}, maintaining a total biofilm density of 50 g L^{-1}, the N_2O formation rates with NOB are higher than if the biofilm is exclusively composed of AOB. This is because NOB have a higher specific rate of oxygen consumption in our model. Based on these considerations, the presence of NOB in a nitrifying biofilm may actually increase N_2O emissions.

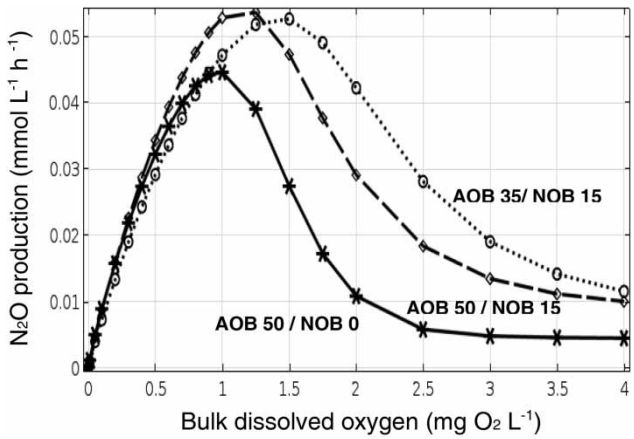

Figure 2 | Emissions from base case 100 μm nitrifying biofilm with AOB and NOB. The presence of nitrite oxidizers (NOB) in the biofilm may enhance the N_2O production. N_2O production rate without NOB (base case, AOB 50 g L^{-1}) and with 15 g L^{-1} NOB (AOB 50 or 35 g L^{-1}).

Effects of gas stripping on N_2O emissions from nitrifying biofilms

In this section, we evaluated the effects of gas flow on both suspended growth (modeled as thin biofilms) and biofilm systems. Results are shown in Figure 3.

Note that our model did not include NO stripping due to aeration. NO stripping can reduce N_2O formation, as NO is a precursor to N_2O. However, our preliminary simulations show that NO is mostly converted to N_2O within the biofilm. NO stripping is more significant for thin biofilms, but these produce little NO due to the lack of substrate gradients.

Research has shown that N_2O can be stripped from suspended growth systems (Rassamee *et al.* 2011; Law *et al.* 2012; Wu *et al.* 2014). Including stripping simply shifts N_2O

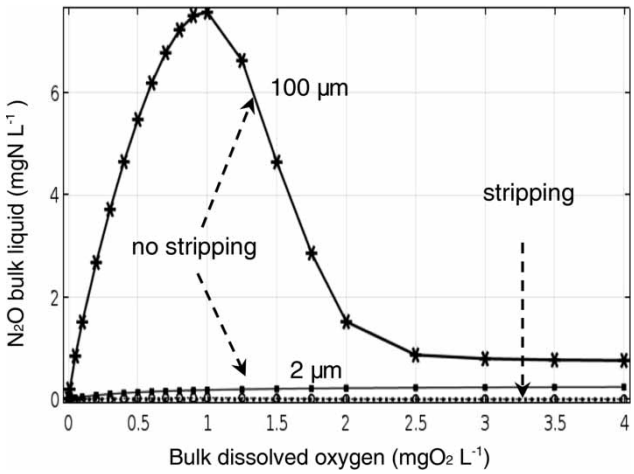

Figure 3 | N_2O bulk liquid concentration for nitrifying conditions as a function of bulk O_2 for a 2 μm suspended growth and 100 μm biofilm system, with stripping (solid line) and without stripping (dashed line).

emissions from the liquid phase to the gas phase (Figure 3). When stripping was included, the N_2O concentration in the liquid phase, for both suspended and biofilm systems, decreased to near-zero levels (Figure 3). But this did not impact N_2O formation rates, since stripping was not linked to aeration and the O_2 concentration remained constant (data not shown). This situation is different for denitrifying bacteria (below), as stripping and biological reduction are competing processes, i.e. more stripping leads to less biological reduction in the biofilm.

Denitrifying biofilms

Effect of O_2 and NO_3^- on N_2O emissions

At low NO_3^- concentrations, emissions from the 5-μm biofilm were higher than the thicker biofilms, but they quickly reached a low maximum rate of N_2O production (Figure 4(a)). This is due to full penetration of NO_3^-. The lower emissions at lower NO_3^- concentrations in the thicker biofilms are explained by the partial NO_3^- penetration within the biofilm depth. Thicker biofilms require higher NO_3^- concentrations to reach maximum denitrification rates throughout the biofilms. For greater biofilm thicknesses, the higher biomass concentration accounted for a higher rate of N_2O formation.

N_2O emissions from 'suspended growth' and biofilm systems were assessed for different O_2 bulk concentrations (Figure 4(b)). At low bulk O_2 concentrations, the amount of N_2O produced per unit reactor volume for the 5-μm 'suspended growth' scenario was higher than the thicker biofilms. Specifically, the 5-μm scenario reached its maximum N_2O emissions at near-zero O_2 concentrations. The N_2O emissions then dropped steeply around 0.1 $mgO_2\ L^{-1}$ and approached zero at around 0.3 mg $O_2\ L^{-1}$. For the 400-μm biofilm, the emissions of N_2O were slightly higher at low bulk O_2

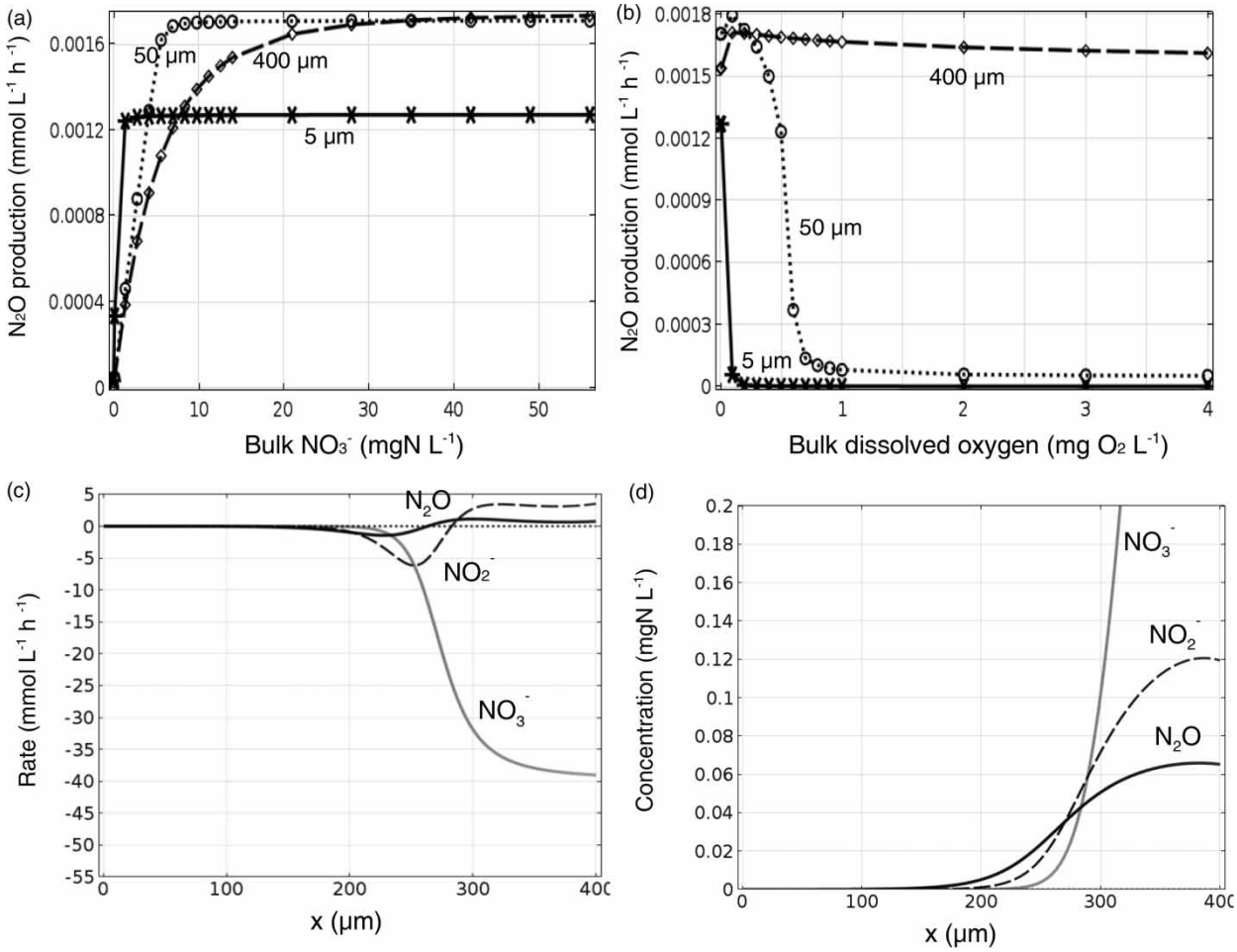

Figure 4 | N_2O production rates for denitrifying biofilms of different thicknesses with a constant biofilm surface area, per unit reactor volume and time, as a function of bulk NO_3^- (a) and bulk O_2 (b). Net component rates over the biofilm depth (x). Results are for the base case conditions with anoxic bulk conditions (net rates of component formation or consumption) (c) and biofilm N-species concentration within biofilm depth (d). Results in (c) and (d) are for the base case conditions with a 400 μm biofilm in the presence of anoxic bulk.

concentrations and then had minimal decrease with increasing O_2. This is due to the O_2 consumption of oxygen in the outer layers, allowing denitrification in the inner layers. In a similar fashion to Figure 4(a) greater biofilm thicknesses, the higher volumetric biomass concentration accounted for higher rate of N_2O formation.

Finally, to better evaluate the mechanisms of N_2O formation in denitrifying biofilms, a base biofilm thickness of 400 μm was considered in more detail (Figure 4(c)). For the 400-μm biofilm with an anoxic bulk, the bulk NO_2^- and N_2O concentrations were 0.12, and 0.07 mgN L^{-1} (Figure 4(d)), respectively (data not shown). When both the NO_3^- concentration and the rate of NO_3^- reduction start to decrease, at around 300 μm, the NO_2^- reduction rate starts to increase and there is a net production of N_2O around 280 μm (data not shown). The inner portion of the biofilm, around 250 μm, has a low concentration of NO_3^- and a higher net NO_2^- consumption rate (Figure 4(c)). In the last region of the biofilm, where NO_3^- is mainly depleted and NO_2^- is at low concentration, the N_2O consumption rate leads the process rates and uses the available electron mediators to reduce N_2O to N_2. Thus, this region is a net sink for N_2O produced in other regions of the biofilm or the bulk.

Effects of stripping on N_2O emissions

The effects of gas stripping were evaluated for a 5-μm system, representing suspended growth, and a 400-μm biofilm system (Figure 5(a)–5(d)). Stripping may occur due to low levels of aeration or due to N_2 gas production. In Figure 5(a)–5(d), we compared N_2O production rates with and without stripping as a function of bulk NO_3^- for both suspended growth and biofilm systems. All these scenarios were tested for non-limiting COD conditions.

For the 5-μm 'suspended growth' biofilm, the maximum N_2O production rate was reached at very low NO_3^-

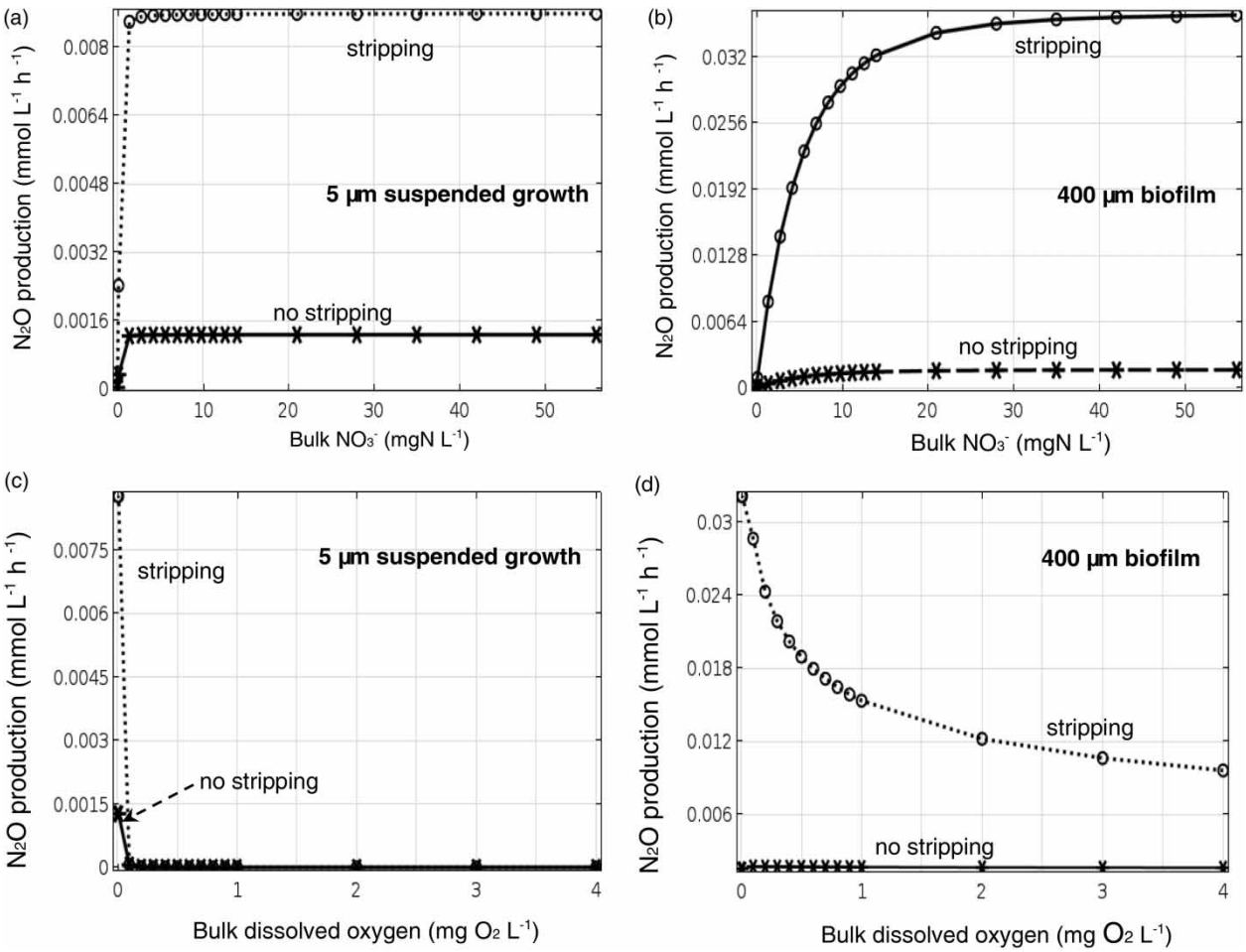

Figure 5 | N_2O production rates in denitrifying biofilms with a constant biofilm surface area, with and without stripping, for a 5-μm biofilm ('suspended growth') (a), (c) and 400-μm biofilm (b), (d) as a function of bulk NO_3^- (a), (b) and (c), (d) as a function of bulk O_2.

concentrations (e.g. 0.1 mgN L^{-1}) (Figure 5(a)). This is because the thin biofilm becomes fully penetrated and saturated by NO_3^- at relatively low bulk concentrations. Stripping increases the N_2O emission by maintaining low bulk N_2O concentrations, which allows the bulk liquid to become a sink for N_2O. Thicker biofilms require a higher NO_3^- concentration to reach the maximum bulk N_2O concentration (Figure 5(b)). Stripping has a greater effect on thicker biofilms (Figure 5(b)).

The effects of gas stripping on N_2O emissions as a function of bulk O_2 were also evaluated (Figure 5(c) and 5(d)). For suspended growth systems (5 μm biofilm) without stripping, no gaseous N_2O emissions occurred throughout the sweep of O_2 concentration for both biofilm and suspended growth. Higher emissions were found when stripping was included for both biofilm and suspended growth (Figure 5(c) and 5(d)). Emissions in this case represent the net emissions; comparing emissions by the formation rate in denitrifying systems would not allow a fair comparison, since denitrifying systems might both produce and consume N_2O. For suspended growth systems, emissions were higher at low O_2. However, they dropped suddenly after the O_2 concentration reached 0.1 mg L^{-1} where a full inhibition of the suspended growth occurred (Figure 5(c)). No emissions occurred afterwards. Biofilms performed differently (Figure 5(d)). They tended to have higher emissions throughout the O_2 sweep. Emissions were highest at low O_2, and decreased when O_2 increased.

CONCLUSIONS

Our model suggests that N_2O emissions from both nitrifying and denitrifying biofilms behave differently from suspended growth systems. In suspended growth systems, all bacteria are exposed to the same bulk concentrations of substrates and intermediates.

As found previously, NH_2OH formed in an aerobic zone of a nitrifying biofilm diffuses to an anoxic zone, resulting in a spike in N_2O formation rates and higher N_2O emissions. However, a novel aspect of this study is that the presence of NOB can also enhance emissions. This was due to the high rate of O_2 reduction by NOB leading to an increase in the O_2 gradient within the biofilm.

Diffusion of intermediates was also important for the denitrifying biofilm, where NO_3^- and NO_2^- reduction govern the activity in the outer portion of the biofilm. Thus, the inner portion of the biofilm has lower concentrations of both compounds, and these can diffuse and be consumed elsewhere. This same aspect applies to N_2O, which can both be exported to the bulk and diffuse towards the deeper regions of a denitrifying biofilm and be reduced.

For denitrifying systems, gas stripping increased emissions by decreasing the amount of N_2O available for reduction in the deeper, anoxic regions of the biofilm. An increase in influent flow rate mimics stripping effects, creating a more pronounced gradient between biofilms and the bulk environment, leading to higher emissions.

These results identify important mechanisms that affect N_2O emissions in nitrifying and denitrifying biofilms. Future research should address the behavior of biofilms containing both nitrifying and denitrifying bacteria, mimicking simultaneous nitrification and denitrification systems.

ACKNOWLEDGEMENTS

F.S. and R.N. were supported by NSF project CBET0954918 (Nerenberg CAREER award) and WERF project U2R10. F.S received additional support from the Bayer Corporation Fellowship. C.P. work was supported by a Melchor Visiting Professor grant from University of Notre Dame. These results were presented at the 5th IWA/WEF Wastewater Treatment Modelling Seminar 2016, Annecy, France (WWTmod2016) seminar and the fruitful discussions are kindly acknowledged.

REFERENCES

Aboobakar, A., Cartmell, E., Stephenson, T., Jones, M., Vale, P. & Dotro, G. 2013 Nitrous oxide emissions and dissolved oxygen profiling in a full-scale nitrifying activated sludge treatment plant. *Water Res.* **47** (2), 524–534.

Ahn, J. H., Kim, S., Park, H., Katehis, D., Pagilla, K. & Chandran, K. 2010 Spatial and temporal variability in atmospheric nitrous oxide generation and emission from full-scale biological nitrogen removal and non-BNR processes. *Water Environ. Res.* **82** (12), 2362–2372.

Colliver, B. & Stephenson, T. 2000 Production of nitrogen oxide and dinitrogen oxide by autotrophic nitrifiers. *Biotechnol. Adv.* **18** (3), 219–232.

CRC Handbook of Chemistry and Physics 2014 95th edn. Section 5: Solubility of selected gases in water. Online at http://www.hbcpnetbase.com/.

Daelman, M. R., van Voorthuizen, E. M., van Dongen, U. G., Volcke, E. I. & van Loosdrecht, M. C. 2015 Seasonal and diurnal variability of N_2O emissions from a full-scale municipal wastewater treatment plant. *Sci. Total Environ.* **1** (536):1–11.

De Beer, D., Schramm, A., Santegoeds, C. M. & Kuhl, M. 1997 A nitrite microsensor for profiling environmental biofilms. *Appl. Environ. Microbiol.* **63** (3), 973–977.

Harper Jr, W. F., Takeuchi, Y., Riya, S., Hosomi, M. & Terada, A. 2015 Novel abiotic reactions increase nitrous oxide

production during partial nitrification: modeling and experiments. *Chem. Eng. J.* **281**, 1017–1023.

Hiatt, W. C. & Grady Jr, C. P. L. 2008 Application of the activated sludge model for nitrogen to elevated nitrogen conditions. *Water Environ. Res.* **80** (11), 2134–2144.

IPCC 2013 *Climate Change 2013: the Physical Science Basis*. Working Group I Contribution to the IPCC 5th Assessment Report. IPCC, Cambridge, UK and New York, NY, USA.

Kampschreur, M. J., Tan, N. C., Kleerebezem, R., Picioreanu, C., Jetten, M. S. & van Loosdrecht, M. C. M. 2007 Effect of dynamic process conditions on nitrogen oxides emission from a nitrifying culture. *Environ. Sci. Technol.* **42**, 429–435.

Kampschreur, M. J., van der Star, W. R. L., Wielders, H. A., Mulder, J. W., Jetten, M. S. M. & van Loosdrecht, M. C. M. 2008 Dynamics of nitric oxide and nitrous oxide emission during full-scale reject water treatment. *Water Res.* **42** (3), 812–826.

Kampschreur, M. J., Temmink, H., Kleerebezem, R., Jetten, M. S. M. & van Loosdrecht, M. C. M. 2009 Nitrous oxide emission during wastewater treatment. *Water Res.* **43**, 4093–4103.

Kampschreur, M. J., Kleerebezem, R., Picioreanu, C., Bakken, L., Bergaust, L., de Vries, S., Jetten, M. S. M. & van Loosdrecht, M. C. M. 2012 Metabolic modeling of denitrification in *Agrobacterium tumefaciens* a tool to study inhibiting and activating compounds for the denitrification pathway. *Frontiers in Microbiol* **3**, 370.

Kimochi, Y., Inamori, Y., Mizuochi, M., Xu, K. & Matsumura, M. 1998 Nitrogen removal and N_2O emission in a full-scale domestic wastewater treatment plant with intermittent aeration. *J. Ferment. Bioeng.* **86** (2), 202–206.

Law, Y., Ni, B. J., Lant, P. & Yuan, Z. 2012 Nitrous oxide (N_2O) production by an enriched culture of ammonia oxidizing bacteria depends on its ammonia oxidation rate. *Water Res.* **46** (10), 3409–3419.

Lu, H. & Chandran, K. 2010 Factors promoting emissions of nitrous oxide and nitric oxide from denitrifying sequencing batch reactors operated with methanol and ethanol as electron donors. *Biotechnol. Bioeng.* **106** (3), 390–398.

Mampaey, K. E., Beuckels, B., Kampschreur, M. J., Kleerebezem, R., van Loosdrecht, M. C. M. & Volcke, E. I. P. 2013 Modelling nitrous and nitric oxide emissions by autotrophic ammonia-oxidizing bacteria. *Environ. Technol.* **34**, 1555–1566.

Ni, B. J. & Yuan, Z. 2015 Recent advances in mathematical modeling of nitrous oxides emissions from wastewater treatment processes. *Water Res.* **15** (87), 336–346.

Ni, B., Ruscalleda, M., Pellicer-Nacher, C. & Smets, B. F. 2011 Modeling nitrous oxide production during biological nitrogen removal via nitrification and denitrification: extensions to the general ASM models. *Environ. Sci. Technol.* **45** (18), 7768–7776.

Ni, B. J., Yuan, Z., Chandran, K., Vanrolleghem, P. A. & Murthy, S. 2013 Evaluating four mathematical models for nitrous oxide production by autotrophic ammonia-oxidizing bacteria. *Biotechnol. Bioeng.* **110**, 153–163.

Ni, B. J., Peng, L., Law, Y., Guo, J. & Yuan, Z. 2014 Modeling of nitrous oxide production by autotrophic ammonia-oxidizing bacteria with multiple production pathways. *Environ. Sci. Technol.* **48** (7), 3916–3924.

Pan, Y., Ye, L., Ni, B. J. & Yuan, Z. 2012 Effect of pH on N_2O reduction and accumulation during denitrification by methanol utilizing denitrifiers. *Water Res.* **46** (15), 4832–4840.

Pan, Y., Ni, B. J. & Yuan, Z. 2013 Modeling electron competition among nitrogen oxides reduction and N_2O accumulation in denitrification. *Environ. Sci. Technol.* **47** (19), 11083–11091.

Picioreanu, C., Van Loosdrecht, M. C. M. & Heijnen, J. J. 1997 Modeling the effect of oxygen concentration on nitrite accumulation in a biofilm airlift suspension reactor. *Water Sci. Technol.* **36** (1), 147–156.

Rassamee, V., Sattayatewa, C., Pagilla, K. & Chandran, K. 2011 Effect of oxic and anoxic conditions on nitrous oxide emissions from nitrification and denitrification processes. *Biotechnol. Bioeng.* **108** (9), 2036–2045.

Sabba, F., Picioreanu, C., Perez, J. & Nerenberg, R. 2015 Hydroxylamine diffusion can enhance N_2O emissions in nitrifying biofilms: a modeling study. *Environ. Sci. Technol.* **49** (3), 1486–1494.

Schreiber, F., Loeffler, B., Polerecky, L., Kuypers, M. M. M. & de Beer, D. 2009 Mechanisms of transient nitric oxide and nitrous oxide production in a complex biofilm. *ISME J.* **3**, 1301–1313.

Schreiber, F., Wunderlin, P., Udert, K. M. & Wells, G. F. 2012 Nitric oxide and nitrous oxide turnover in natural and engineered microbial communities: biological pathways, chemical reactions, and novel technologies. *Front. Microbiol.* **3**, 372.

Soler-Jofra, A., Stevensa, B., Hoekstraa, M., Picioreanu, C., Sorokin, D., van Loosdrecht, M. C. M. & Pérez, J. 2016 Importance of abiotic hydroxylamine conversion on nitrous oxide emissions during nitritation of reject water. *Chem. Eng. J.* **287**, 720–726.

Stewart, P. S. 2003 Diffusion in biofilms. *J. Bacteriol.* **185** (5), 1485–1491.

Tallec, G., Garnier, J., Billen, G. & Gousailles, M. 2006 Nitrous oxide emissions from secondary activated sludge in nitrifying conditions of urban wastewater treatment plants: effect of oxygenation level. *Water Res.* **40**, 2972–2980.

Wanner, O., Eberl, H. J., Morgenroth, E., Noguera, D., Picioreanu, C., Rittmann, B. E. & Van Loosdrecht, M. C. M. 2006 IWA Task Group on Biofilm Modeling. Mathematical Modeling of Biofilms. IWA Scientific and Technical Report No. 18, IWA Publishing.

Wu, G., Zheng, D. & Xing, L. 2014 Nitritation and N_2O emission in a denitrification and nitrification two-sludge system treating high ammonium containing wastewater. *Water* **6** (10), 2978–2992.

Wunderlin, P., Mohn, J., Joss, A., Emmenegger, L. & Siegrist, H. 2012 Mechanisms of N_2O production in biological wastewater treatment under nitrifying and denitrifying conditions. *Water Res.* **46** (4), 1027–1037.

Ye, L., Ni, B.-J., Law, Y., Byers, C. & Yuan, Z. 2014 A novel methodology to quantify nitrous oxide emissions from full-scale wastewater treatment systems with surface aerators. *Water Res.* **48**, 257–268.

First received 31 May 2016; accepted in revised form 30 September 2016. Available online 14 October 2016